

# Synthesis, Solid-Phase Reaction, and Patterning of Acid-Labile 3,4-Ethylenedioxythiophene-Based Conjugated Polymers

Jianfei Yu and Steven Holdcroft\*

Department of Chemistry, Simon Fraser University, Burnaby, BC, Canada, V5A 1S6

Received February 5, 2002. Revised Manuscript Received June 3, 2002

3,4-Ethylenedioxythiophene (EDOT)-based conjugated polymers bearing tetrahydropyranyl side groups were synthesized. These include poly[(3-(2-(2-tetrahydropyranyloxy)ethyl)-thiophene)-(3,4-ethylenedioxythiophene)] (PTHPET-EDOT), and poly[(3-(11-(2-tetrahydropyranyloxy)undecyl)thiophene)-(3,4-ethylenedioxythiophene)] (PTHPUDT-EDOT). PTHPUDT-EDOT exhibits an enhanced stability in its oxidized state and a high optical contrast ratio between its reduced and oxidized states. Despite its rigid-rod nature, PTHPUDT-EDOT undergoes an acid catalytic reaction that leads to the cleavage and complete elimination of the tetrahydropyranyl group. The decrease in solubility of the deprotected polymer allows for the deposition of PTHPUDT-EDOT in a spatially controlled fashion using chemically amplified photolithography and soft lithography.

## Introduction

$\pi$ -Conjugated polymers ( $\pi$ CPs) are promising materials with which to fabricate organic microelectronic, optoelectronic, and electrooptic devices such as thin film field-effect transistors,<sup>1</sup> photovoltaics,<sup>2</sup> light-emitting devices,<sup>3</sup> and electrochromic windows.<sup>4</sup> When compared to inorganic counterparts,  $\pi$ CPs possess intrinsic advantages, such as ease of preparation, processability, flexibility, low density, and potentially low cost. Moreover, they are versatile and their properties can be fine tuned.<sup>5</sup>

Polythiophene is an important class of  $\pi$ CPs. However, unsubstituted polythiophene is insoluble and infusible due to the rigidity of the backbone and strong intermolecular interactions. A soluble form of polythiophene can be prepared by the introduction of alkyl side chains.<sup>6</sup> The flexible side chain reduces polymer–polymer intermolecular interactions and increases polymer–solvent interactions. The side chains can also be chosen so that soluble polymers can be rendered insoluble after chemical or photochemical reaction.<sup>7</sup> This

transition allows for the spatial deposition of  $\pi$ CPs for device fabrication.

The electronic and optical properties of  $\pi$ CPs can be tuned by molecular engineering. The properties can be controlled to some degree by the size, structure, and electronic properties of the side chain substituents. For example, substitution at the 3-position with an alkyl chain having more than four carbons causes the resultant poly(3-alkylthiophene) to form highly ordered lamellar structures with strong  $\pi$ -stacking; a desirable feature for their application in organic FETs.<sup>8</sup> Conversely, substitution at both the 3- and 4-positions causes adjacent thiophene rings to twist with respect to each other, thus inhibiting  $\pi$ -stacking; a structure favored for organic LEDs.<sup>9</sup> Recently, it was reported that such structural derivatization and fine-tuning can be achieved by postfunctionalization of precursor polythiophenes.<sup>10</sup>

Poly(3,4-ethylenedioxythiophene) (PEDOT) is a good example of a molecular engineered  $\pi$ CP.<sup>11</sup> Here, a dioxane ring is fused onto thiophene with the oxygen directly attached at the 3- and 4-positions. It may be expected that disubstitution would cause the conjugated backbone to twist and reduce the effective conjugation,<sup>12</sup> but in PEDOT, this effect is alleviated. Moreover, the oxygen atoms exert an electron-donating effect that

\* To whom all correspondence should be addressed.

(1) (a) Sirringhaus, H.; Tessler, N.; Friend, R. H. *Science* **1998**, *280*, 1741. (b) Bao, Z.; Dodabalapur, A.; Lovinger, A. J. *Appl. Phys. Lett.* **1996**, *69*, 4108. (c) Brown, A. R.; de Leeuw, D. M.; Havinga, E. E.; Pomp, A. *Synth. Met.* **1994**, *68*, 65.

(2) (a) Halls, J. J. M.; Walsh, C. A.; Greenham, N. C.; Marsegila, E. A.; Friend, R. H.; Moratti, S. C.; Holmes, A. B. *Nature* **1995**, *376*, 498.

(3) Burroughes, J. H.; Bradley, D. D. C.; Brown, A. R.; Marks, R. N.; MacKay, K.; Friend, R. H.; Burns, P. L.; Holmes, A. B. *Nature*, **1990**, *347*, 539.

(4) (a) Rauth, R. D. *Electrochim. Acta* **1999**, *44*, 3165. (b) Pennisi, A.; Simone, F.; Barletta, G.; Di Marco, G.; Lanza, L. *Electrochim. Acta* **1999**, *44*, 3237. (c) Schottland, P.; Zong, K.; Gaupp, C. L.; Thompson, B. C.; Thomas, C. A.; Giurgiu, I.; Hickman, R.; Abboud, K. A.; Reynolds, J. R. *Macromolecules* **2000**, *33*, 7051.

(5) (a) Skotheim, T. A., Ed.; *Handbook of Conducting Polymers*; Marcel Dekker: New York, 1986. (b) Roncali, J.; *Chem. Rev.* **1997**, *97*, 173.

(6) (a) Jen, K.-Y.; Miller, G. G.; Elsenbaumer, R. L. *J. Chem. Soc., Chem. Commun.*, **1986**, 1346. (b) Sugimoto, R.; Takeda, S.; Gu, H. B.; Yoshino, K. *Chem. Express* **1986**, *1*, 635.

(7) Lowe, J.; Holdcroft, S. *Macromolecules* **1995**, *28*, 4608.

(8) (a) Bao, Z.; Lovinger, A. J. *Chem. Mater.* **1999**, *11*, 2607. (b) Bao, Z.; Dodabalapur, A.; Lovinger, A. J. *Appl. Phys. Lett.* **1996**, *69*, 4108.

(c) Sirringhaus, H.; Tessler, N.; Friend, R. H. *Science* **1998**, *280*, 1741. (c) Sirringhaus, H.; Brown, P. J. *Nature* **1999**, *401*, 685.

(9) (a) Yang, C.; Abley, M.; Holdcroft, S. *Macromolecules* **1999**, *32*, 6889. (b) Politis, J. K.; Curtis, M. D.; Gonzalez, L.; Martin, D. C.; He, Y.; Kanicki, J. *Chem. Mater.* **1998**, *10*, 1713.

(10) Li, Y.; Vamvounis, G.; Yu, J.; Holdcroft, S. *Macromolecules* **2001**, *34*, 3130.

(11) (a) Groenendaal, L.; Jonas, F.; Freitag, D.; Pielartzik, H.; Reynolds, J. R. *Adv. Mater.* **2000**, *12*, 481. (b) Heywang, G.; Jonas, F. *Adv. Mater.* **1992**, *4*, 116. (c) Dietrich, M.; Heinze, J.; Heywang, G.; Jonas, F. *J. Electroanal. Chem.* **1994**, *369*, 87.

(12) McCullough, R. D.; *Adv. Mater.* **1998**, *10*, 93. (b) Andersson, M.; Thomas, O.; Mammo, W.; Svensson, M.; Theander, M.; Inganäs, O. *J. Mater. Chem.* **1999**, *9*, 1933.

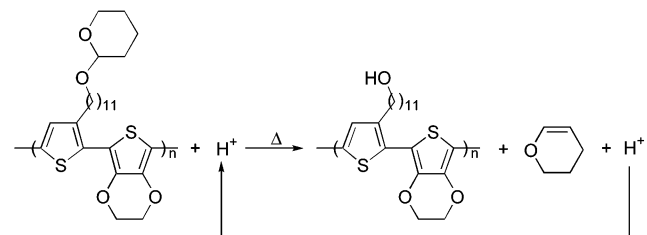
raises the HOMO level of the conjugated system and reduces the band gap. As a result, PEDOT exhibits a lower oxidation potential and higher stability in its oxidized state compared to other substituted polythiophenes. EDOT can also be incorporated into other conjugated moieties in order to tailor electronic and optical properties. For example, replacing thiophene in polyvinylthienylene with EDOT reduces the band gap of the polymer to 1.4 eV;<sup>13</sup> coupling EDOT with electron-accepting conjugated moieties, such as thieno-[3,4-*b*]pyrazine<sup>14</sup> and 4-dicyanomethylene-4*H*-cyclopenta[2,1-*b*;3,4-*b*']dithiophene,<sup>15</sup> produces  $\pi$ CPs with band gaps of <0.36 eV; coupling EDOT with 2,5-dialkoxyphenylene produces  $\pi$ CPs possessing band gaps (1.75–2.0 eV) much lower than their unsubstituted thiophene analogues.<sup>16</sup>

Thus, PEDOT and related polymers have emerged as one of the most promising class of  $\pi$ CPs, and numerous applications have been realized or are proposed. These include antistatic coatings,<sup>11a</sup> electrode materials for solid electrolyte capacitors,<sup>17</sup> hole-injecting layers,<sup>18</sup> transparent electrodes for organic LEDs,<sup>19</sup> and electrochromic materials.<sup>20</sup> A drawback of PEDOT, however, is its poor solubility and processability. This can be circumvented by derivatizing them with alkyl side chains.<sup>11b,20b,21</sup> These derivatives retain their relatively low band gap and, as electrochromic materials, exhibit faster redox switching, a higher degree of electrochromic contrast, and higher durability than the parent PEDOT. Long alkyl side chain ( $\geq$  octyl) substituents solubilize PEDOT, which enables it to be prepared on a larger scale.<sup>21a</sup>

Parallel to interest in EDOT-based polymers, is a growing interest in depositing  $\pi$ CPs in a spatially controlled fashion for device applications. Many reports describe the application of photolithography to control the deposition of  $\pi$ CPs. These are based on photo-cross-linking, photoinduced doping/dedoping, and photoinduced structure transformation.<sup>22</sup> There are also reports of non-photolithographic patterning techniques, includ-

- (13) Fu, Y.; Cheng, H.; Elsenbaumer, R. L. *Chem. Mater.* **1997**, *9*, 1720.
- (14) Akoudad, S.; Roncali, J. *Chem. Commun.* **1998**, 2081.
- (15) Huang, H.; Pickup, P. G. *Chem. Mater.* **1998**, 2212.
- (16) Wang, F.; Wilson, M. S.; Rauch, R. D.; Schottland, P.; Thompson, B. C.; Reynolds, J. R. *Macromolecules* **2000**, *33*, 2083.
- (17) (a) Kudoh, Y.; Akami, K.; Matsuya, Y. *Synth. Met.* **1999**, *102*, 973. (b) Chosh, S.; Inganäs, O. *Adv. Mater.* **1999**, *11*, 1214.
- (18) (a) Brown, T. M.; Kim, J. S.; Cacialli, F.; Friend, R. H.; Daik, R.; Feast, W. J. *Appl. Phys. Lett.* **1999**, *75*, 1679. (b) Kim, J. S.; Cacialli, F.; Friend, R. H. *Appl. Phys. Lett.* **1999**, *74*, 3084. (c) Kim, J. S.; Cacialli, F.; Friend, R. H.; Daik, R.; Feast, W. J. *Synth. Met.* **1999**, *102*, 1065. (d) Kim, J. S.; Granström, M.; Friend, R. H.; Johansson, N.; Salaneck, W. R.; Daik, R.; Feast, W. J.; Cacialli, F. *J. Appl. Phys.* **1998**, *84*, 6859. (e) Cao, Y.; Yu, G.; Zhang, C.; R. Menon; Heeger, A. J. *Synth. Met.* **1997**, *87*, 171. (f) Xing, K. Z.; Fahland, M.; Chen, X. W.; Inganäs, O.; Salaneck, W. R. *Synth. Met.* **1997**, *89*, 161. (g) Granström, M.; Berggren, M.; Inganäs, O. *Synth. Met.* **1996**, *76*, 141. (h) Granström, M.; Berggren, M.; Inganäs, O. *Science* **1995**, *267*, 1497. (i) Bharathan, J.; Yang, Y. *J. Appl. Phys.* **1998**, *84*, 3201.
- (19) Granlund, T.; Nyberg, T.; Roman, L. S.; Svensson, M.; Inganäs, O. *Adv. Mater.* **2000**, *12*, 269.
- (20) (a) Sapp, S. A.; Sotzing, G. A.; Reddinger, J. L.; Reynolds, J. R.; *Adv. Mater.* **1996**, *8*, 808. (b) Sotzing, G. A.; Reddinger, J. L.; Reynolds, J. R.; Steel, P. J. *Synth. Met.* **1997**, *84*, 199. (c) Sankaran, B.; Reynolds, J. R. *Macromolecules* **1997**, *30*, 2582. (d) Sapp, S. A.; Sotzing, G. A.; Reynolds, J. R. *Chem. Mater.* **1998**, *10*, 2101. (e) Gustafsson, J. C.; Inganäs, O.; Andersson, M.; Booth, C.; Azens, A.; Granqvist, C. G. *Electrochim. Acta* **1995**, *40*, 2233.
- (21) (a) Kumar, A.; Reynolds, J. R. *Macromolecules* **1996**, *29*, 7629. (b) Hovinga, E. E.; Mutsaers, C. M. J.; Jenneskens, L. W. *Chem. Mater.* **1996**, *8*, 769.

**Scheme 1. Acid-Catalyzed Elimination of Dihydropyran from PTHPUTD-EDOT**



ing soft lithography,<sup>23</sup> ink jet printing,<sup>24</sup> and screen printing.<sup>25</sup> Recently, an acid-sensitive polythiophene derivative, poly(3-(2-tetrahydropyranoyloxy)ethyl)thiophene (PTHPET), was patterned with micron resolution by chemically amplified photolithography (CAP).<sup>26</sup> Here, the tetrahydropyranyl group (THP) is photochemically converted to a hydroxy group by acid catalysis,<sup>26,27</sup> changing the polymers' solubility. Due to the catalytic nature of the deprotection reaction, the process possesses a high photosensitivity. It was also found that copolymerization of 3-(2-tetrahydropyranoyloxy)ethyl-thiophene with 3-hexythiophene allows for modification of the conditions required for the solid-state reaction to occur.<sup>28</sup>

In an effort to develop a prototypical polymer that possesses both EDOT functionality (for properties of low band gap and low oxidation potential) and acid-labile functionality (for patterning purposes), we synthesized the first soluble, acid-sensitive EDOT-based polymer, poly[(3-(11-(2-tetrahydropyranoyloxy)undecyl)-thiophene)-(3,4-ethylenedioxythiophene)] (PTHPUDT-EDOT).<sup>29</sup> This polymer undergoes the solid-state, acid-catalyzed reaction shown in Scheme 1 and was used to demonstrate chemically amplified soft lithography of a  $\pi$ CP. In this paper, the detailed synthesis, characterization, and patterning are reported. Furthermore, to develop an understanding of structure–property relationships of these polymers, we report on THP-protected analogues, poly(3-(2-tetrahydropyranoyloxy)ethyl)thiophene (PTHPET) and poly(3-(11-(2-tetrahydropyranoyloxy)undecyl)thiophene (PTHPUDT).

## Experimental Section

**Measurements.** 400 MHz  $^1$ H NMR spectra were obtained in CDCl<sub>3</sub> (400 MHz Bruker AMX400). Molecular weight and

- (22) Holdcroft, S. In *Handbook of Organic Conductive Molecules and Polymers*; Nalwa, H. S., Ed.; John Wiley & Sons: Chichester, 1997; Vol. 4.
- (23) (a) Xia, Y.; Rogers, J. A.; Paul, K. E.; Whitesides, G. M. *Chem. Rev.* **1999**, *99*, 1823. (b) Xia, Y.; Whitesides, G. M. *Angew. Chem., Int. Ed. Engl.* **1998**, *37*, 550. (c) Rogers, J. A.; Bao, Z.; Meier, M.; Dodabalapur, A.; Schueller, O. J. A.; Whitesides, G. M. *Synth. Met.* **2000**, *115*, 5. (d) Beh, W. S.; Kim, I. T.; Qin, D.; Xia, Y.; Whitesides, G. M. *Adv. Mater.* **1999**, *11*, 1038.
- (24) (a) Wu, C. C.; Macry, D.; Lu, M. H.; Sturm, J. C. *Appl. Phys. Lett.* **1998**, *72*, 519. (b) Hebner, T. R.; Sturm, J. C. *Appl. Phys. Lett.* **1998**, *73*, 1775. (c) Bharathan, J.; Yang, Y. *Appl. Phys. Lett.* **1998**, *72*, 2660.
- (25) Garnier, F.; Hajlaoui, R.; Yassar, A.; Srivastava, P. *Science*, **1994**, *265*, 1684. (b) Bao, Z.; Feng, Y.; Dodabalapur, A.; Raju, V. R.; Lovinger, A. J. *Chem. Mater.* **1997**, *9*, 1299. (c) Bao, Z.; Rogers, J. A.; Katz, H. E. *J. Mater. Chem.* **1999**, *9*, 1895.
- (26) (a) Yu, J.; Abley, M.; Yang, C.; Holdcroft, S. *Chem. Commun.* **1998**, 1503. (b) Yu, J.; Holdcroft, S. *Macromolecules* **2000**, *33*, 5073.
- (27) (a) Murray, K. A.; Moratti, S. C.; Baigent, D. R.; Greenham, N. C.; Pichler, K.; Holmes, A. B.; Friend, R. H. *Synth. Met.* **1995**, *69*, 395. (b) Murray, K. A.; Holmes, A. B.; Moratti, S. C.; Friend, R. H. *Synth. Met.* **1996**, 161.
- (28) Yu, J.; Orfino, F.; Holdcroft, S. *J. Mater. Chem.* **2000**, *13*, 526.
- (29) Yu, J.; Holdcroft, S. *Chem. Commun.* **2001**, 1274.

its distribution were determined using a GPC (Waters Model 510), equipped with a  $\mu$ -Styrgel column, and/or using MALDI-MS (Voyager-DE Biospectrometry) and dithranol (Aldrich) as the matrix. Elemental analyses were performed by using an EA 110 elemental analyzer. Chemical ionization (CI) and electron impact (EI) mass spectra were carried out using a HP-5985 GC-MS.

Polymer film samples were prepared by casting polymers on glass or Si wafers from chloroform solution in the absence or presence of camphorsulfonic acid. For X-ray diffraction (XRD) measurements, acid-free samples were annealed at  $\sim 130$   $^{\circ}$ C for 20 min for PTHPET and PTHPUTD, and  $\sim 180$   $^{\circ}$ C under  $N_2$  for 20 min for PTHPUTD-EDOT. The acid-catalyzed deprotection was carried out by heating the samples at  $\sim 170$  for 20 min. UV-vis absorption spectra were obtained using a Cary 3E (Varian) spectrophotometer. Differential scanning calorimetry (DSC) measurements were carried out on 5–10 mg of polymer using a Perkin-Elmer DSC-7 calorimeter and a scan rate of 10  $^{\circ}$ C/min under a  $N_2$ . Thermogravimetric analysis (TGA) was performed on 3–5 mg of polymer sample under ambient atmosphere using a Shimadzu TGA-50 thermogravimetric analyzer. Infrared spectra were recorded using a Bomem Michelson FTIR (120 series). Small-angle X-ray diffraction analysis was carried out using a D/MAX-RAPID (Rigaku) X-ray microdiffraction system with a X-ray tube generator, a copper target ( $\lambda_{K\alpha} = 1.542$   $\text{\AA}$ ) and an image plate detector. Data were collected in reflection mode. Molecular-scale calculations were performed using Hyperchem software (Hypercube Inc.). Interlamellar spacings were estimated from all-trans coplanar geometries and contour lengths of fully extended side chains. The diameter of the tetrahydropyranloxy group (THP) was determined on the basis of its chair conformation. Conductivity was measured by the four-point probe technique. Polymer films were doped by 0.1 M ferric chloride solution in nitromethane or 0.1 M silver triflate in ether. The quantity of camphorsulfonic acid deposited by soft lithography on stamp surfaces was determined indirectly by spiking the acid solution with anthracene and quantifying it using UV spectroscopy. The quantity of acid in polymer films was determined using FTIR.

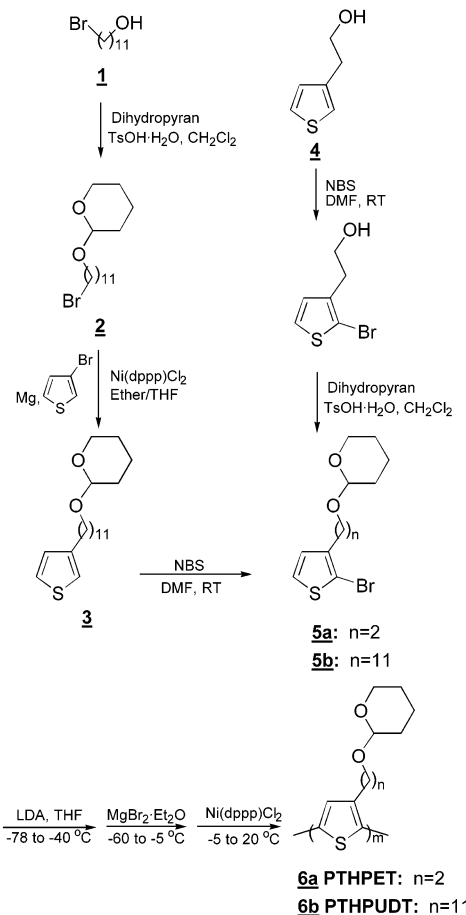
**Photolithography.** Photolithography was performed on films spin cast on glass substrates from chloroform solutions containing polymer and the photoacid generator (PAG), *N*-(camphorsulfonyloxy)-1,8-naphthalimide. Photolysis of the PAG by exposure to UV light through a direct contact chrome-on-glass mask generated a latent acid image in the polymer film. The polymeric pattern was obtained by heating the film at 165  $^{\circ}$ C for 2.5 min and development with chloroform. A 1000 W Xe lamp (Oriel) was employed as the UV light source. The wavelength of incident was selected using a 361 nm broadband filter.

**PDMS Stamp.** An elastomeric stamp of PDMS was molded from a photoresist-patterned template. The template was prepared by spin casting a positive photoresist on a 4 in. diameter wafer and patterning by photolithography. The stamp was molded by pouring a prepolymer of PDMS (Sylgard 184) onto the template and curing at 60  $^{\circ}$ C overnight.

## Results and Discussion

**Synthesis.** THP-containing homopolymers and EDOT analogues were synthesized from their corresponding brominated monomers or bithiophene monomers using the Grignard cross-coupling method.<sup>30</sup> Scheme 2 illustrates the synthetic route for PTHPET (6a)<sup>26</sup> and PTHPUTD (6b). To prepare 2-bromo-3-(11-(2-tetrahydropyranloxy)undecyl)thiophene (5b), 11-bromo-1-undecanol (1) was protected by reaction with excess dihydropyran. This was coupled to 3-bromothiophene to afford 3-(11-(2-tetrahydropyranloxy)undecyl)th-

**Scheme 2. Synthetic Scheme for PTHPET and PTHPUTD**

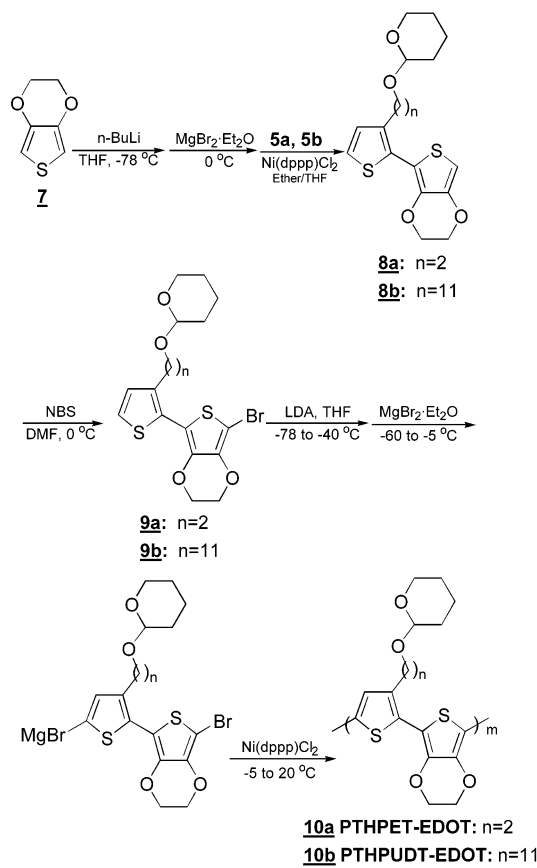


iophene (3), which was selectively brominated using NBS. Scheme 3 illustrates the synthetic route for PTHPET-EDOT (10a) and PTHPUTD-EDOT (10b). Bithiophene monomers 8a and 8b were prepared by coupling the brominated THP-containing monomers 5a and 5b with the Grignard reagent prepared from EDOT (7). Selective bromination of 8a and 8b at the  $\alpha$ -position was achieved by reaction with NBS at 0  $^{\circ}$ C to yield 9a,b. EDOT-based polymers were prepared by condensation of the brominated bithiophene monomers.

Unlike PTHPUTD-EDOT, PTHPET-EDOT is barely soluble in common solvents. Sufficient concentration was obtained for UV-vis absorption and GPC analysis, but it was not sufficient to cast thick polymer films for investigation of solid-state reaction. Solid-state reaction was therefore restricted to PTHPUTD-EDOT. Molecular weight, polydispersity index, and wavelength of maximum absorption are shown in Table 1.

<sup>1</sup>H NMR spectroscopy of PTHPUTD-EDOT showed characteristic resonance peaks at 4.56 and 2.73 ppm, assigned to the methine protons of THP and the  $\alpha$ -methylene protons of the side chain, respectively. The ethylene proton peak corresponding to the EDOT units occurred at 4.36 ppm. The molecular weight of 5500 Da determined by GPC is higher than that determined by MALDI ( $M_w = 4000$  Da), presumably because the former is based on hydrodynamic volume and the polymers are relatively stiff. Three major subpeaks were found in the MALDI spectrum (figure available in the Supporting Information). The various peaks correspond to polymers

(30) McCullough, R. D.; Lowe, R. D.; Jayaraman, M.; Anderson, D. L. *J. Org. Chem.* **1993**, *58*, 904.

**Scheme 3. Synthetic Scheme for PTHPET-EDOT and PTHPUTD-EDOT****Table 1. Characteristics of THP-Protected Homopolymers and Their Corresponding EDOT-Based Polymers**

polymer	$M_w$	$M_n$	D	$\lambda_{\max}$ (nm)	
				CHCl <sub>3</sub>	film
PTHPET ( <b>6a</b> )	19 900	10 700	1.85	439	467
PTHPUTD ( <b>6b</b> )	22 100	14 200	1.56	449	520
PTHPET-EDOT ( <b>10a</b> ) <sup>a</sup>	1 800	1 500	1.20	507	535
PTHPUTD-EDOT ( <b>10b</b> )	5 500	4 200	1.31	569	570
	4 000 <sup>b</sup>	3 300 <sup>b</sup>	1.20 <sup>b</sup>		
P3HT	16 300	11 300	1.44	449	520

<sup>a</sup> Soluble portion. <sup>b</sup> Determined by MALDI.

possessing H/H, H/Br, and Br/Br termini, which result from metal–halogen exchange between different polymer chains.<sup>31</sup> The mass difference between two blocks of subpeaks, 478 Da, corresponds to the repeat unit mass of THPUTD-EDOT.

**Optical Properties.** Optical absorption spectra are shown in Figure 1. PTHPET exhibits a  $\lambda_{\max}$  of 439 and 467 nm in solution and solid state, respectively. These are much lower than regioregular poly(3-alkylthiophene)s, e.g., P3HT (449 nm, solution; 520 nm, film), due to strong steric interactions between juxtaposed thiophenyl rings possessing bulky THP groups. This interaction is alleviated to a degree by distancing the THP group from the backbone. Thus the  $\lambda_{\max}$  of PTHPUTD is similar to that of P3HT. In contrast to PTHPET, the absorption spectrum of PTHPUTD films show fine

structure, which is an indication of a larger degree of coplanarity and ordering. When EDOT is coupled with THPET,  $\lambda_{\max}$  (507 nm, solution; 535 nm, solid state) red shifts compared to that of PTHPET, due to the electron-donating effect of the ethylenedioxy substituent. Similarly, the absorption spectrum of PTHPUTD-EDOT is red-shifted compared to PTHPUTD. The  $\lambda_{\max}$  of PTHPUTD-EDOT films is 570 nm with a low-energy shoulder at 622 nm. The band gap, estimated from the low-energy absorption edge, is 1.67 eV, which is similar to that of PEDOT films (1.6–1.7 eV).<sup>11a</sup> PTHPUTD-EDOT in solution exhibits a similar absorption spectrum to the film and also exhibits fine structure. It can be inferred that the polymer is relatively rigid and may even form colloidal aggregates in solution,<sup>32</sup> as reported for  $\pi$ CPs such as polyoctylfuran.<sup>33</sup> In summary, PTHPUTD-EDOT exhibits similar optical properties to PEDOT, yet is readily soluble.

**Oxidative Doping.** Solutions of PTHPUTD-EDOT are deep purple. When  $\text{FeCl}_3$  is added (25 to 30 mol % based on the thiophenyl unit), PTHPUTD-EDOT is oxidized, and the color of the solution is pale gray. Oxidation is instantaneous (<1 s). Oxidation of PTHPUTD and PTHPET solutions are sluggish (>~3 h to complete). A 100 nm thick PTHPUTD-EDOT film is oxidized in 2–3 s in the presence of 0.1 M  $\text{FeCl}_3$ , whereas, the same reaction takes 2–3 min for PTHPET and PTHPUTD films. The rapidity of the oxidation reaction of PTHPUTD-EDOT is due to its low oxidation potential. Oxidatively doped films of PTHPUTD-EDOT possess a lower absorbance in the visible region than PTHPET and PTHPUTD films (UV-vis spectra of doped films available in the Supporting Information). PTHPUT-EDOT films are deep purple when neutral and a highly transmissive pale gray color when oxidatively doped (figure available in the Supporting Information). PTHPUTD-EDOT exhibits a high optical contrast at  $\lambda_{\max}$  570 nm. For example, the transmittance of a ~150 nm film increased from 10% in its neutral state to 74% in its oxidized state. Table 2 lists transmittance data at two different wavelengths.

Electrical conductivity was measured through 60–90 nm thick films oxidatively doped with either silver triflate or iron chloride (Table 3). The conductivity of PTHPUTD-EDOT is marginally higher than that of PTHPET, lower than that of PTHPUTD, and similar to that P3HT and alkyl-substituted PEDOT derivatives (PEDOT-C<sub>6</sub>).<sup>21b</sup> However, EDOT-based polymers are significantly more stable. The time required for the conductivity to decline to half its initial value was 1600 and 720 h for films of PTHPUTD-EDOT oxidized with  $\text{AgOTf}$  and  $\text{FeCl}_3$ , respectively. This is 20 and 30 times longer than PTHPET and PTHPUTD.

**Solid-State Structure.** Figure 2 shows X-ray diffraction (XRD) patterns of three THP-protected polymers. PTHPET yields a peak at  $2\theta = 5.05$  (see Figure 3a),<sup>28</sup> which corresponds to an interlamellar *d* spacing of 17.5 Å along the *a* axis. Although the THP group does not completely prevent PTHPET from achieving molec-

(31) (a) Liu, J.; Loewe, R. S.; McCullough, R. D. *Macromolecules* **1999**, *32*, 5777. (b) Boymond, L.; Rottlander, M.; Cahiez, G.; Knochel, P. *Angew. Chem., Int. Ed. Engl.* **1998**, *37*, 1701.

(32) Yamamoto, T.; Komarudin, D.; Arai, M.; Lee, B.-L.; Suganuma, H.; Asakawa, N.; Inoue, Y.; Kubota, K.; Sasaki, S.; Fukuda, T.; Matsuda, H. *J. Am. Chem. Soc.* **1998**, *120*, 2047.

(33) Politis, J. K.; Nemes, J. C.; Curtis, M. D. *J. Am. Chem. Soc.* **2001**, *123*, 2537.

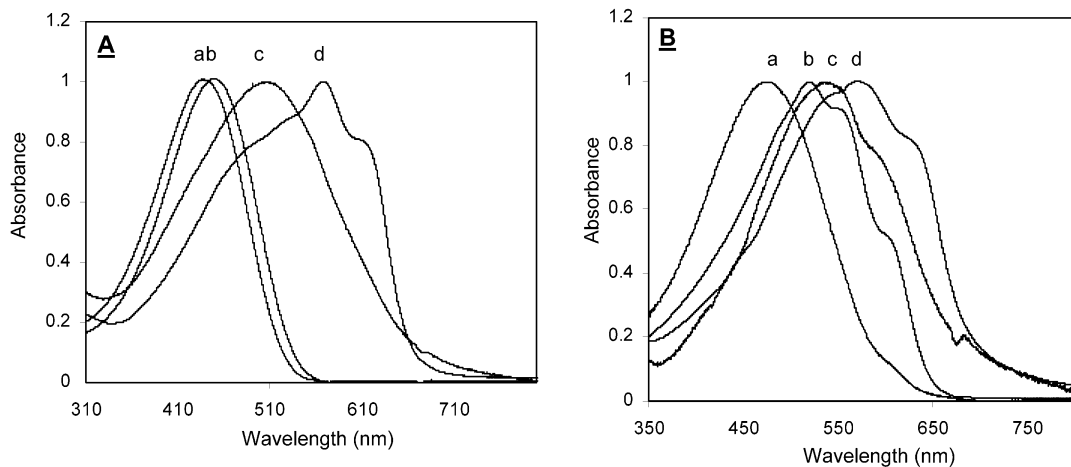


**Figure 1.** UV-vis spectra of polymers in  $\text{CHCl}_3$  (A) and as films (B): (a) PTHPET, (b) PTHPUDT, (c) PTHPET-EDOT, and (d) PTHPUDT-EDOT.

**Table 2. Optical Contrast of Polymers between Reduced and Oxidized States**

polymers	T(%, 400 nm)		T(%, $\lambda_{\text{max}}$ )		T(%, 700 nm)		color	
	neut	oxid	neut	oxid	neut	oxid	neut	oxid
PTHPET	25	41	10	57	97	35	orange	gray
PTHPUDT	50	51	10	59	93	37	purple	gray
PTHPUDT-EDOT	52	51	10	74	67	66	deep purple	pale gray

**Table 3. Conductivity and Stability of Polymers in the Oxidized State**

polymer film	AgOTf-oxidized		FeCl <sub>3</sub> -oxidized	
	conductivity (s/cm)	half-life (h)	conductivity (s/cm)	half-life (h)
PTHPET	18	60	4	18
PTHPUDT	30	79	27	26
PTHPUDT-EDOT	20	1600	12	720
PEDOT-C <sub>6</sub> <sup>a</sup>	40 <sup>b</sup>			

<sup>a</sup> Poly(3,4-(octylenedioxy-1,2)-thiophene).<sup>21b</sup> <sup>b</sup> Electronically oxidized film.<sup>21b</sup>

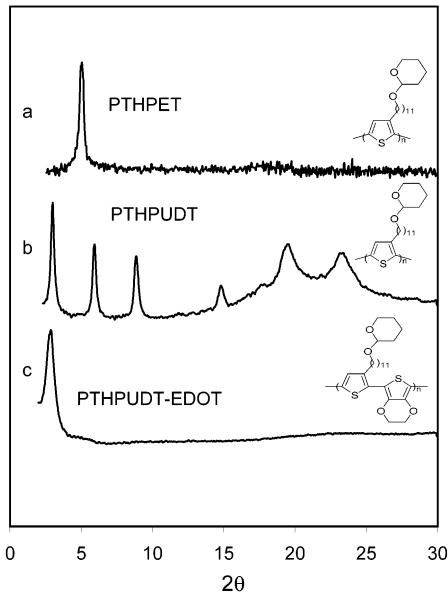


**Figure 2.** XRD plots of (a) PTHPET, (b) PTHPUDT, and (c) PTHPUDT-EDOT.

ular ordering, the degree of order is relatively low, as evidenced by the absence of higher order peaks. PTHPUDT, possessing longer side chains, shows strong first-, second-, and third-order peaks at  $2\theta = 3.00^\circ$ ,

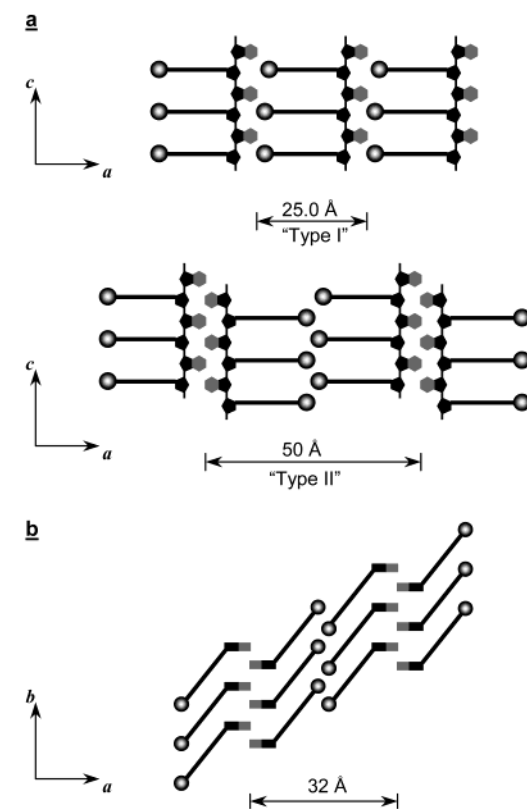


**Figure 3.** Possible lamellar structures of PTHPUDT-EDOT: nontilted (a) and tilted (b) side chains.

5.94°, and 8.90°, respectively (Figure 2b). These represent an  $a$ -axis  $d$  spacing of 29.4 Å. The lower intensity peaks at 12.1°, 14.9°, and 18.0° are attributed to fourth-, fifth-, and sixth-order diffractions. Two broad peaks, observed at  $2\theta = 23.6^\circ$  and  $19.5^\circ$ , represent  $d$  spacings of 3.81 and 4.55 Å, respectively. The former is typical of interchain  $\pi$ -stacking. The latter is considered to originate from crystallization of alkyl side chains<sup>34,35</sup> Compared to PTHPET, PTHPUDT possesses a higher

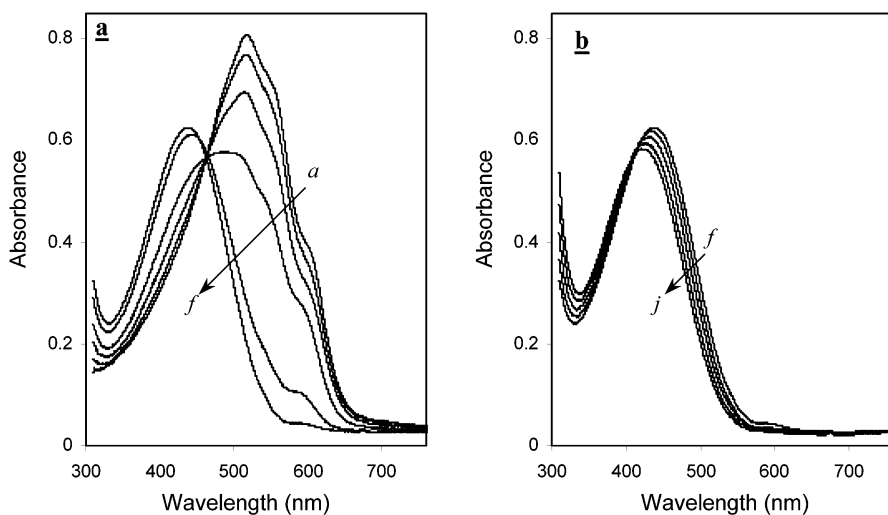


**Figure 4.** Thermochromism of PTHPUTD: (a) 20, (b) 40, (c) 60, (d) (80), (e) 100, (f) 120, (g) 140, (h) 160, (I) 180, and (j) 200 °C.

degree of crystallinity, which implies that it adopts a more planar conformation. It has been suggested that the observation of a XRD peak due to  $\pi$ -stacking correlates with the observation of fine structure in their absorption spectra.<sup>33</sup> The fact that PTHPET films do not exhibit fine structure, whereas PTHPUTD does, is consistent with this correlation.

PTHPUTD-EDOT gives rise to a single XRD peak at  $2\theta = 2.75^\circ$ , indicating a periodic ordering of 32.1 Å (Figure 2c). No peaks due to higher order diffractions or interchain  $\pi$ -stacking are present. These observations do not correlate with UV-vis spectra, since fine structures are clearly observed in PTHPUTD-EDOT solutions and films. The absence of the higher order XRD peaks may be attributed to the low degree of ordering, a consequence of the high rigidity of the polymer. Indeed, a freshly prepared PTHPUT-EDOT film did not show any diffraction peak until annealed at 180 °C. Alternatively, a low degree of ordering may result from different sizes of the substituents<sup>36</sup> and the variation of interlamellar distances.<sup>37</sup>

Assuming an all-trans, fully extended side chain with adjacent thiophenes possessing a coplanar conformation, the interlamellar *d* spacings for PTHPET and PTHPUTD were computed to be 19 and 42 Å, respectively, i.e., larger than the experimental values of 17.5 and 29.0 Å. The THP group is ~5.1 Å in diameter; therefore, interdigitation of THP-containing side chains is unlikely. The actual *d* spacing of PTHPET and PTHPUTD is most likely due to tilting of the side chains,<sup>38</sup> because this helps the side chain achieve a 4.5 Å hexagonal close packing arrangement.<sup>39</sup>

PTHPUTD-EDOT possesses alternate THPUTD and EDOT groups. The two different size substituents may produce two possible lamellar-like structures, as illustrated in Figure 3a. The “type I” lamellar structure is disqualified by the fact that the computed interlamellar *d* spacing is 25 Å, a value much smaller than the experimental value (32.1 Å). In the absence of interdigitation (“type II” structure, tilting absent), the *d* spacing is computed to be 50 Å, which is larger than the measured value. PTHPUTD is thus presumed to adopt a “type II” lamellar structure in which the side chains are tilted as illustrated in the Figure 3b.

Temperature-dependent absorption spectra provide insight into molecular organization. It has been observed that some films of poly(3-alkylthiophene)s undergo a continuous color change with increasing temperature.<sup>40</sup> For example, the absorption maximum of P3HT is blue-shifted from 520 nm (room temperature) to 430 nm (200 °C). It has been reported that PTHPET exhibits a similar thermochromic pattern to P3HT, except the blue shift occurs from 467 to 427 nm. This phenomenon has been rationalized by the twisting of the polymer backbone at elevated temperature and a subsequent decrease in the effective conjugation length. Shown in Figure 4 are the absorption spectra of PTHPUTD. Close examination of the spectra reveals that (a) from 20 to 60 °C, the band centered at 520 nm decreases in intensity and progressively blue shifts (Figure 4a); (b) at 80 °C, this band undergoes a more substantial blue shift and exhibits an isosbestic point at 450 nm (Figure 4a); (c) between 100 and 120 °C, a new band at 430 nm increases in intensity (Figure 4a); (d) between 120 and 200 °C, this new band undergoes a moderate blue shift and decreases in intensity (Figure 4b). The observation that PTHPUTD exhibits a nearly constant  $\lambda_{\max}$  between 20 and 80 °C is attributed to its dense morphology and side chain crystallization. The isosbestic point observed at 80° is also evidence of side chain crystallization.<sup>40</sup> A first order melting transition in this temperature region converts the semicrystalline state to a disordered phase. A further increase in temperature causes an incremental decrease in the effective conjugation length and a continuous blue shift.

(34) Yamamoto, T.; Xu, Y.; Inoue, T.; Yamaguchi, I. *J. Polym. Sci.: Part A: Polym. Chem.* **2000**, *38*, 1493.

(35) (a) Watanabe, J.; Harkness, B. R.; Sone, M.; Ichimura, H. *Macromolecules* **1994**, *27*, 507. (b) Hsieh, H. W. S.; Post, B.; Morawetz, H. *J. Polym. Sci., Polym. Phys. Ed.* **1976**, *14*, 124.

(36) (a) Ofer, D.; Swager, T. M.; Wrighton, M. S. *Chem. Mater.* **1995**, *7*, 418. (b) Swager, T. M. In *Organised Molecular Assemblies in the Solid State*; Whitesell, J. K., Ed.; John Wiley & Sons: New York, 1999; Chapter 2.

(37) Roe, R.-J. In *Methods of X-ray and Neutron Scattering in Polymer Science 2000*; Oxford University Press: Chichester, 1999.

(38) (a) Prosa, T. J.; Winokur, M. J.; Moulton, J.; Smith, P.; Heeger, A. J. *Synth. Met.* **1993**, *55*–57, 370. (b) Tashiro, K.; Ono, K.; Minagawa, Y.; Kobayashi, K.; Kawai, T.; Yoshino, K. *J. Polym. Sci., Polym. Phys. Ed.* **1991**, *29*, 1223.

(39) Prosa, T. J.; Winokur, M. J.; Moulton, J.; Smith, P.; Heeger, A. J. *Macromolecules* **1992**, *25*, 363.

(40) Yang, C.; Orfino, F. P.; Holdcroft, S. *Macromolecules* **1996**, *29*, 6510.

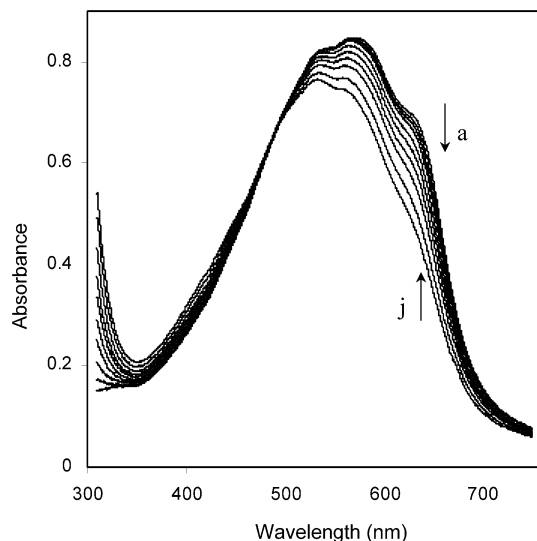


**Figure 5.** Thermochromism of PTHPUTD-EDOT: (a) 20, (b) 40, (c) 60, (d) (80), (e) 100, (f) 120, (g) 140, (h) 160, (i) 180, and (j) 200 °C.

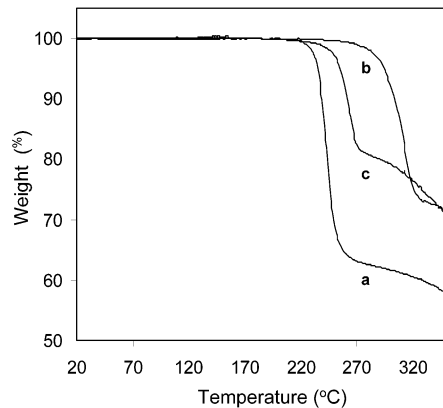


**Figure 6.** TGA thermograms of (a) PTHPET, (b) PTHPUTD, and (c) PTHPUTD-EDOT in the absence of acid.

In contrast to PTHPUTD, PTHPUTD-EDOT undergoes a minor decrease in intensity and only a slight blue shift between 20 and 200 °C (Figure 5).

**Solid-State Reaction.** PTHPET undergoes an efficient deprotection reaction in the absence or presence of acid.<sup>26</sup> It is found that PTHPUTD and PTHPUTD-EDOT also undergo thermolytic deprotection with ~100% completeness, as illustrated by TGA (Figure 6) and DSC (figure available in the Supporting Information). In the absence of acid, the TGA thermogram of PTHPUTD-EDOT shows an 18% loss in mass between 240 and 270 °C. The theoretical weight loss is 17.6%. The thermogram of PTHPUTD yields a 25% weight loss between 275 and 325 °C (theoretical value, 24.8%). DSC thermograms of acid free samples give rise to a large endothermic peak in the same temperature regions. These peaks are attributed to the thermal deprotection of polymer films with concomitant vaporization of DHP.

Solid-state reactions in polymers are affected by polymer morphology, structure, and molecular weight. Thus, different deprotection temperatures are observed for the same reaction in three different polymers. In the absence of acid, the onset temperature for deprotection is 220, 275, and 235 °C, for PTHPET, PTHPUTD, and PTHPUTD-EDOT, respectively. The higher deprotec-

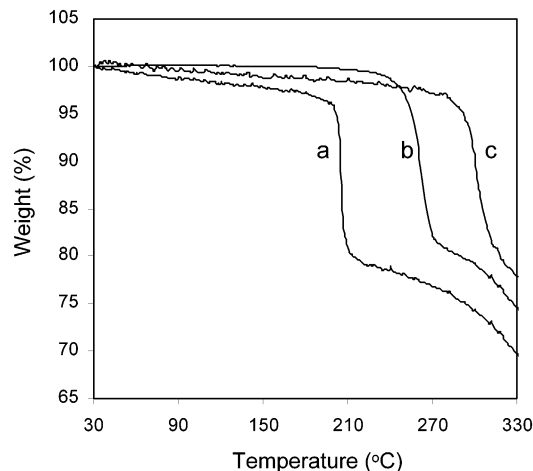


**Figure 7.** TGA thermograms of PTHPUTD-EDOT possessing different molecular weight ( $M_w$ ), (a) 3300, (b) 4000, and (c) 5500 g/mol, in the absence of acid.

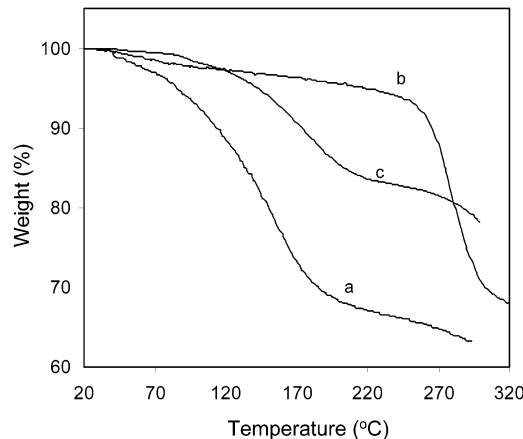


**Figure 8.** TGA thermograms of (a) PTHPET, (b) PTHPUTD, and (c) PTHPUTD-EDOT in the presence of 5 mol % camphorsulfonic acid.

tion of PTHPUTD is attributed to its much longer side chains and denser morphology. The molecular weight PTHPUTD-EDOT was significantly lower than the other two polymers, and the effect of molecular weight was unknown. To examine the effect of molecular weight on the deprotection temperature, PTHPUTD-EDOT polymers with different molecular weight were prepared. Shown in Figure 7 is the effect of the molecular weight of PTHPUTD-EDOT on the TGA thermograms. The deprotection temperature increases with molecular weight. In this case, longer polymers impose stronger intermolecular interactions.

Shown in Figure 8 are TGA thermograms of PTHPET, PTHPUTD, and PTHPUTD-EDOT ( $M_w = 4000$  g/mol) in the presence of 5% camphorsulfonic acid (mol % based on the thiényl unit). Deprotection of PTHPUTD-EDOT (Figure 8c) occurs at a temperature 150 °C lower than in the presence of acid. The observed weight loss is ~16% and occurs with only 5 mol % acid, thus providing evidence that the reaction is acid catalyzed. PTHPUTD (see Figure 8b), however, shows only a small decrease in deprotection temperature in the presence of acid, for reasons discussed below.

Upon heating PTHPUTD-EDOT ( $M_w = 4000$  g/mol) films in the presence of 5 mol % camphorsulfonic acid at ~170 °C for 20 min, the XRD-determined  $d$  spacing

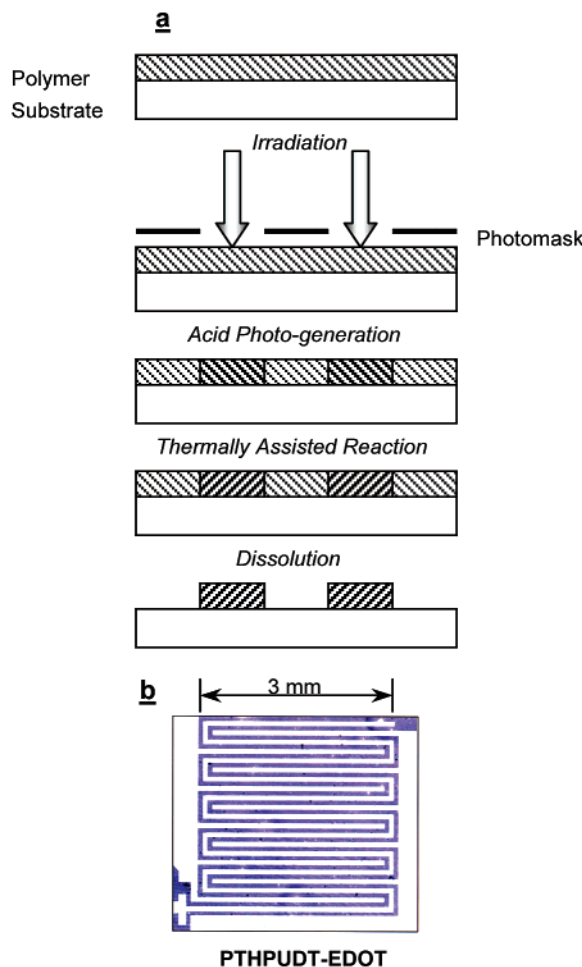


**Figure 9.** (a) Scheme depicting chemically amplified photolithographic process and (b) a micrograph of patterned PTH-PUDT-EDOT.

decreased from 32.1 to 28.8 Å (figure available in the Supporting Information), due to the elimination of the THP group and densification. Structural transformation of the polymer was accompanied by the emergence of a large FTIR peak at  $\sim 3400\text{ cm}^{-1}$ , attributed to the formation of terminal hydroxyl groups;<sup>27</sup> a decrease in signals at 2923 and 2852  $\text{cm}^{-1}$ , corresponding to loss of THP-methylenes; and a dramatic decrease in solubility.

**Chemically Amplified Photolithography.** Application of the acid-catalyzed deprotection reaction is demonstrated in chemically amplified photolithography as illustrated in Figure 9. Films of PTH-PUDT-EDOT (60 nm) containing 30% of *N*-(camphorsulfonyloxy)-1,8-naphthalimide were irradiated through a photomask with filtered (361 nm broadband filter) UV light from a 1000 Xe lamp. The irradiation intensity and irradiation dose was 0.80  $\text{mW cm}^{-2}$  and  $\sim 500\text{ mJ cm}^{-2}$ , respectively. Irradiation of the photoacid generator produces a latent acid image of camphorsulfonic acid, but no acid-catalyzed deprotection reaction of PTH-PUDT-EDOT was detected until the film is heated. The irradiated film was subsequently heated to 165 °C for 2.5 min and developed with  $\text{CHCl}_3$  to dissolve unexposed polymer, whereupon a negative image of the photomask was obtained. An interdigitated pattern of the imaged polymer (dark region) is shown in Figure 9b.

**Chemically Amplified Soft Lithography.** Chemically amplified soft lithography of conjugated polymer

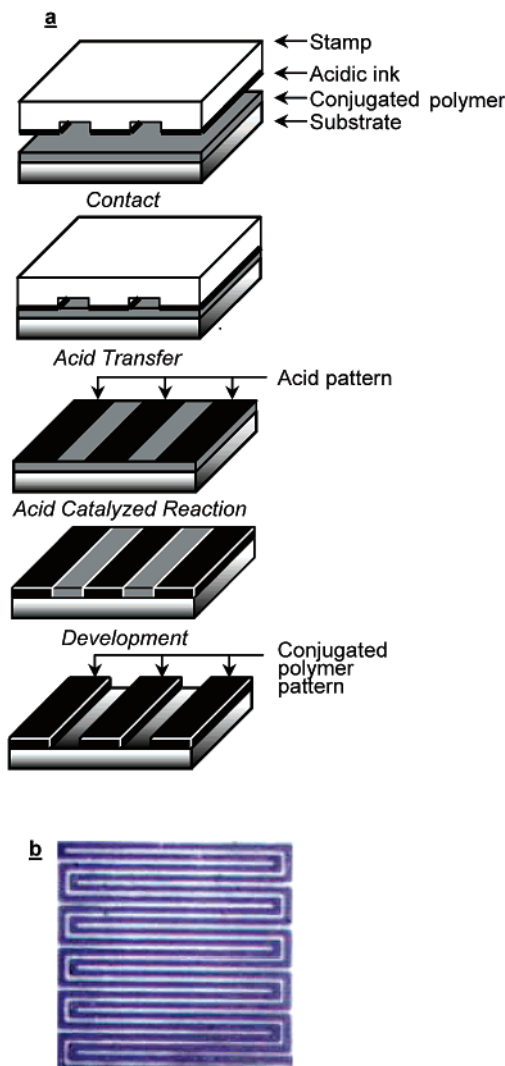


**Figure 10.** (a) Scheme depicting chemically amplified soft lithographic process and (b) a micrograph of patterned PTH-PUDT-EDOT.

draws on the concepts of both chemical amplification and soft lithography. Figure 10a shows a scheme of the procedure. The patterning of PTH-PUDT-EDOT via acid-catalyzed chemistry was achieved by spatial deposition of the acid onto the surface of a PTH-PUDT-EDOT film (90 nm thick), followed by heating and development. PTH-PUDT-EDOT was spin cast onto a glass substrate from a chloroform solution. An "acidic ink", comprising of 0.01 M camphorsulfonic acid in tetrahydrofuran and hexane (50/50), was applied to a PDMS stamp by contact for 3 s. The "inked" stamp was allowed to dry in air for 30 s and then pressed lightly on top of the polymer film for 10–15 s, thereby transferring the acid to its surface. Thermal treatment of the film at 130 °C for 10 s resulted in cleavage and elimination of THP in the regions where acid was deposited. These regions were rendered insoluble by virtue of the residual hydroxy group and the change in polarity. Development in chloroform provided a positive image of the stamp, as shown in Figure 10b.

To determine the quantity of acid transferred to the polymer by microcontact printing, a series of experiments were carried out using much larger areas of PDMS in conjunction with UV-vis and FTIR spectro-

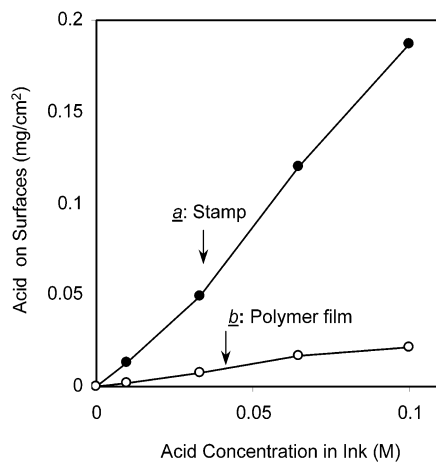


**Figure 11.** Acid loading on (a) stamp and (b) polymer film as the function of camphorsulfonic acid concentration in acidic ink.

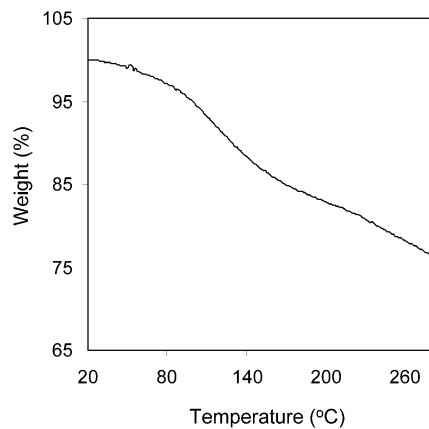


**Figure 12.** TGA thermogram of PTHPUDT-EDOT coated with ~20 mol % camphorsulfonic acid.

scopic analysis, as described in the Experimental Section. Figure 11 shows the quantity of acid picked up by stamp and transferred to the polymer surface during the printing process as a function of acid concentration in the “acidic ink”. For a concentration of 0.01 M, i.e., that used for imaging purpose, it was found that  $2.1 \mu\text{g}/\text{cm}^2$  of acid is transferred onto the surface of the polymer film. The molar ratio of acid to the thiényl ring is calculated to be  $\sim 1:4$  for a film of thickness  $\sim 90 \text{ nm}$ . This confirms that the reaction is catalytic in acid and therefore chemically amplified. The achievement of chemically amplified in a polymeric film via printed acid was further confirmed by TGA analysis. Camphorsulfonic acid (20 mol %) was deposited on PTHPUDT-EDOT polymer films ( $\sim 1 \mu\text{m}$  thick) by solution casting.

Figure 12 shows the resulting TGA thermogram illustrating a weight loss at a temperature significantly lower than the polymer in the absence of acid.

The effect of acid concentration on the patterning of PTHPUDT-EDOT was investigated. Shown in Figure 13 are patterned polymer images obtained using 0.003, 0.010, and 0.033 M acid solutions. A 0.010 M acid solution provided a uniform polymer pattern (Figure 13b), but the 0.003 M solution yielded a discontinuous polymeric pattern (Figure 13a) due to incomplete deprotection of the polymer. With a larger acid concentration, e.g., 0.033 M, undesired bridging between adjacent parallel line structures occurred (Figure 13c), due to the acid catalytic reaction extending well beyond the zones of deposition.

This soft lithographic process eliminates possible damage to the conjugated polymer structure due to irradiation. Here, the UV spectra of the PTHPUDT-EDOT films before and after patterning (figure available in the Supporting Information) are similar. Furthermore, the doping of the polymeric pattern with oxidants results in an instantaneous color change from deep purple to transparent pale gray with a highly increased transmittance, indicating its potential suitability for patterned electrochromic devices.

## Conclusions

THP-containing, EDOT-based polymers, PTHPET-EDOT and PTHPUDT-EDOT, have been synthesized by Grignard cross-coupling reaction of 3,4-ethylenedioxy-3'-(2-(2-tetrahydropyranyloxy)ethyl)-2,2'-bithiophene and 3,4-ethylenedioxy-3'-(11-(2-tetrahydropyranyloxy)ethyl)-2,2'-bithiophene. Although PTHPET is soluble, PTHPET-EDOT is not. Solubility is achieved by increasing the side chain length of the THP-containing unit. PTHPUDT-EDOT is soluble and exhibits good film-forming properties. PTHPUDT-EDOT possesses the properties of a low band gap conjugated polymer, e.g. facile oxidation, high stability in the oxidized state, and high optical contrast between the neutral and oxidized states. PTHPUDT-EDOT possesses long-rang order in the solid state, but the degree of ordering is low compared to other regioregular polymers. Although PTHPUDT is reluctant to undergo the acid-catalyzed deprotection reaction because of its crystallinity, this occurs readily with PTHPUDT-EDOT both at high temperature in absence of acid and at much lower temperature in the presence of acid. The action of acid is catalytic. PTHPUDT-EDOT can be patterned by chemically amplified photolithography and soft lithography.

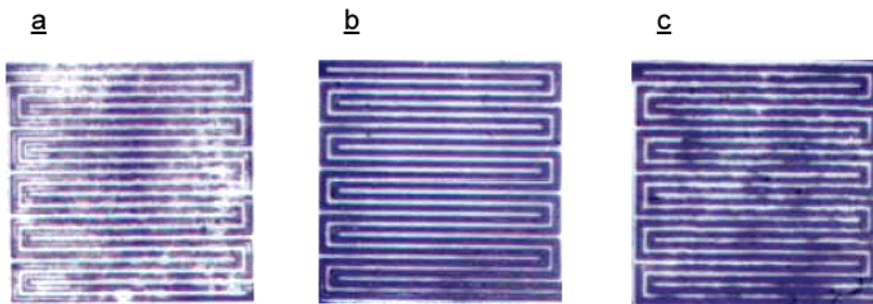


**Figure 13.** Micrographs of PTHPUDT-EDOT patterned by chemically amplified soft lithography using acidic inks containing various acid concentrations of (a) 0.003, (b) 0.010, and (c) 0.033 M.

**Acknowledgment.** We thank the Natural Sciences and Engineering Research Council of Canada for financial support.

**Supporting Information Available:** Synthetic procedures for the preparation of monomers and polymers, images

of PTHPUDT-EDOT films in neutral and doped states, and selected MALDI, DSC, XRD, UV-vis data are provided (CIF). This material is available free of charge via the Internet at <http://pubs.acs.org>.

CM020113C